Heterogeneity of the early outward current in ventricular cells isolated from normal and hypertrophied rat hearts

Jean-Pierre Benitah, Ana Maria Gómez, Patrick Bailly, Jean-Philippe da Ponte, Guy Berson, Carmen Delgado, Paco Lorente

Journal of Physiology (1993), **469**, *pp.* 111–138
With 9 figures
Printed in Great Britain

HETEROGENEITY OF THE EARLY OUTWARD CURRENT IN VENTRICULAR CELLS ISOLATED FROM NORMAL AND HYPERTROPHIED RAT HEARTS

BY JEAN-PIERRE BÉNITAH*, ANA MARIA GOMEZ†, PATRICK BAILLY*, JEAN-PHILIPPE DA PONTE*, GUY BERSON*, CARMEN DELGADO† AND PACO LORENTE*

*From *U195 INSERM Faculté de Médecine, 63001 Clermont-Ferrand, France and the †Instituto de Farmacología y Toxicología (CSIC), Universidad Complutense, 28040 Madrid, Spain*

(Received 23 June 1993)

SUMMARY

1. The nature, magnitude and kinetics of the 4-aminopyridine-sensitive early outward current (I_{to}) were analysed in isolated ventricular myocytes from the septum, the apex and the left ventricular free wall of rat ventricles using the whole-cell voltage clamp method. The modulatory effect of pressure overload-induced cardiac hypertrophy on the regional variations of I_{to} was assessed in each topographical class of cells.

2. Voltage clamp experiments were performed at room temperature (20–25 °C) in the absence of Na^+ on both sides of the membrane and in the presence of 3 mM $CoCl_2$. I_{to} was studied from a holding potential of −80 mV and determined by subtraction of total outward currents elicited by the same protocols in the presence of 3 mM 4-aminopyridine (4-AP) from those obtained in its absence.

3. In normal hearts, membrane passive properties were very similar in each topographical class of cells. Our results confirmed that the predominant early outward current in rat ventricular cells was 4-AP-sensitive, time and voltage dependent, and demonstrated that the magnitude of the current varied on a regional basis: current density of I_{to} in left ventricular free wall cells ($30{\cdot}1 \pm 9{\cdot}2$ pA/pF at +60 mV) was larger than in apex cells ($20{\cdot}2 \pm 1{\cdot}7$ pA/pF) or in septum cells ($11{\cdot}9 \pm 3{\cdot}3$ pA/pF). We noticed a larger variability in data from left ventricular free wall compared with other regions.

4. No shift in steady-state voltage dependence of I_{to} activation and inactivation was found. However, the maximal computed chord conductances were (in μS/pF): $0{\cdot}18 \pm 0{\cdot}07$ for left ventricular free wall cells, $0{\cdot}13 \pm 0{\cdot}02$ for apex cells, and $0{\cdot}08 \pm 0{\cdot}02$ for septum cells. These findings might reflect a differential distribution in functional channel densities.

5. No difference in voltage-dependent I_{to} activation kinetics was present with respect to topography. However, inactivation time constants in septum were longer than those of both other groups.

6. Left ventricular hypertrophy was induced by abdominal aortic constriction and

its effects compared to the findings from normal rats. Hypertrophied cells had similar resting potentials but higher capacitance values than normal cells. Although I_{to} magnitude appeared not to be modified, the current density–voltage curves were slightly shifted to more positive potentials and significantly decreased as compared to normal cells (in pA/pF, at +60 mV): 8·4 ± 5·0 in the left free wall group, 11·6 ± 2·0 in the apex group, and 3·8 ± 1·5 in the septum group. Steady-state activation and inactivation parameters were not clearly modified, but kinetics were slowed down.

7. We conclude, therefore, that I_{to} is differentially distributed among different regions of the normal rat ventricle and we propose that this regional heterogeneity may be related to different distributions of functional channel densities, rather than alterations in whole-cell kinetics or single-channel properties. Pressure overload-induced hypertrophy reduces I_{to} current availability by decreasing current densities without any significant change of whole-cell kinetics, while a homogenizing tendency of the ionic profile is observed among the studied regions. One possible explanation for the hypertrophy-induced variations may be an absence of I_{to} channel neosynthesis, leading to a decrease of channel density per surface area unit.

INTRODUCTION

A transient outward current was originally shown in sheep cardiac Purkinje fibres clamped to membrane potentials positive to −20 mV (Deck & Trautwein, 1964) and for a long time it was considered to be a unique feature of this tissue related to rapid phase 1 repolarization (Fozzard & Hiraoka, 1973; Coraboeuf & Carmeliet, 1982). In recent years, with the improvement of patch clamp techniques, a wealth of experimental data has shown the presence of a transient outward current in other cardiac tissues from various species (Gintant, Cohen, Datyner & Kline, 1991), and has demonstrated the role of this current in initiating the repolarization of action potentials (Tseng, Robinson & Hoffman, 1987). Magnitude and even existence of the current are strongly dependent on a number of factors, such as the considered species (Josephson, Sanchez-Chapula & Brown, 1984), maturational changes during development (Escande, Loisance, Planche & Coraboeuf, 1985; Kilborn & Fedida, 1990), regional differences in the distribution of the electrical properties (Giles & Imaizumi, 1988; Furukawa, Myerburg, Furukawa, Bassett & Kimura, 1990; Fedida & Giles, 1991), and pathology (Antzelevitch *et al.* 1991).

We have recently reported that in septal human ventricular myocytes isolated from patients with pressure overload-induced cardiac hypertrophy, the slow inward current is largely dominant compared to the outward currents. In contrast to the observations in human atrial cells (Escande, Coulombe, Faivre, Deroubaix & Coraboeuf, 1987), the transient outward current in hypertrophic human ventricular myocytes was very reduced or absent (Bénitah, Bailly, D'Agrosa, Da Ponte, Delgado & Lorente, 1992*a*). Since the presence of a transient outward current has not yet been established with any certainty in the human ventricle, and due to the absence of control data, it remains to be seen whether this pattern is related to regional differences in the properties of the cells or whether it is due to the pathological condition of the patients.

A differential distribution of transient outward currents in epicardial and endocardial layers or among different portions of ventricular tissue, has been initially

assumed on the basis of action potential data (Antzelevitch *et al.* 1991; Watanabe, Delbridge, Bustamente & McDonald, 1983). Recently reported voltage clamp data have lent support to this assumption by showing that transient outward currents are significantly greater in epicardial than in endocardial cells dissociated from cat and rabbit left ventricles (Furukawa *et al.* 1990; Fedida & Giles, 1991).

In pressure overload-induced cardiac hypertrophy, the regulatory mechanisms of the action potential configuration are severely impaired. An increase in the duration of the action potential is the most commonly observed disturbance in the hypertrophied myocardium from rats with renal hypertension (Keung & Aronson, 1981), from cats submitted to pulmonary artery constriction (Tritthart, Leudcke, Bayer, Stierle & Kaufmann, 1975), and from guinea-pigs subjected to a progressive aortic banding (Nordin, Siri & Aronson, 1989). The question then arises as to which membrane currents are involved in these pathophysiological processes. This question is, however, currently a matter of considerable debate among electrophysiologists. Keung (1989) has previously stated that the action potential lengthening in hypertrophied rat myocardium is due to an increase in peak current density and a slower inactivation of I_{Ca}. But other investigators have presented experimental evidence in favour of the assumption that the action potential lengthening in myocardial hypertrophy is more probably due to a decrease in an early outward current rather than in an alteration in the magnitude or kinetics of I_{Ca} (Kleiman & Houser, 1988; Scamps, Mayoux, Charlemagne & Vassort, 1990).

These considerations have prompted us to assess the role of the physiological heterogeneity of ventricular wall and the pressure overload-induced cardiac hypertrophy on the magnitude and kinetics of the 4-aminopyridine-sensitive early outward current in rat ventricle. The rat heart was regarded as an appropriate model of ventricular wall heterogeneity since it exhibits a 4-aminopyridine-sensitive early outward current whose amplitude is much larger than in other species (Josephson *et al.* 1984). This large early outward current is composed of transient and maintained components (Dukes & Morad, 1991; Apkon & Nerbonne, 1991), and plays a prominent role in the control of amplitude and duration of the action potential plateau (Josephson *et al.* 1984) particularly during the initial phase of repolarization (Kilborn & Fedida, 1990). Moreover, this current seems to be responsible for some of the heterogeneous electrical properties of ventricular tissue (Keung & Aronson, 1981; Watanabe *et al.* 1983; Antzelevitch *et al.* 1991). Accordingly, to simulate the human cardiac hypertrophy subsequent to aortic stenosis, we performed our studies on rat hypertrophied ventricles after abdominal aortic constriction.

The purpose of this paper is to improve our understanding of the heterogeneity within the ventricular wall of adult rat hearts. The following questions were addressed. (i) Which type of differential distribution for I_{to} is physiologically present in septum, apex and left ventricular free wall as observed in isolated rat ventricular myocytes? (ii) How can this physiological pattern be altered by cardiac hypertrophy induced by pressure overload?

Our results demonstrate the existence of a differential distribution of I_{to} in the aforementioned regions of rat hearts, and a consistent modulation of the physiological heterogeneity as a prominent feature of the cardiac hypertrophic process.

Preliminary results have been presented in abstract form (Bénitah *et al.* 1992*b*).

METHODS

Cell isolation

Data were obtained from thirteen adult male Sprague–Dawley rats (weight 380–495 g). Left ventricular myocytes were enzymatically dissociated through the use of a collagenase-based dispersion technique derived from the procedure described previously by Powell, Terrar & Twist (1980). After intraperitoneal injection of 4 IU/g heparin, the animal was killed by decapitation and the heart was quickly removed, weighed and mounted on a Langendorff apparatus for retrograde perfusion of the coronary circulation. The heart was first washed out for 2 min with a Tyrode solution gassed with 100% O_2 at 35 °C, and then perfused with a nominally calcium-free Tyrode solution until beating stopped (within 1–2 min). The Tyrode solution contained (mM): NaCl, 140; KCl, 5·4; NaH_2PO_4, 0·4; $NaHCO_3$, 5·8; $MgCl_2$, 1; $CaCl_2$, 1·8; glucose, 22; and Hepes, 5; pH was adjusted to 7·4 with NaOH. The preparation was next exposed for 16·5 min/(g of heart weight) to 60 IU/ml collagenase (Worthington, type II) dissolved in the calcium-free Tyrode solution. Thereafter collagenase was washed out for 3 min with a 'Kraftbrühe' (KB) solution containing (mM): KCl, 30; KH_2PO_4, 10; $MgCl_2$, 0·5; taurine, 15; glucose, 11; EGTA, 0·5; glutamate, 70; and Na_2ATP, 5; with a pH adjusted to 7·4 with KOH. The perfusion rate was adjusted to 10 ml/min with a peristaltic pump, except during the time exposure to the recirculating enzyme in which the flow rate was 8 ml/min. After removing the atria, the ventricles were carefully dissected in three anatomical parts: the septum, the apex, and the left ventricular free wall, while the right ventricular free wall was discarded; this partition allowed us to define three groups: the septum, the apex, and the left ventricular free wall cells. Each portion was separately cut off and gently stirred to obtain cells. Isolated myocytes were then filtered through a 250 μm nylon mesh and centrifuged for 4 min at 20 *g*. The pellets were finally suspended and stored for 30 min before experiments in the storage solution containing (mM): NaCl, 117; KCl, 5·7; KH_2PO_4, 1·5; $NaHCO_3$, 4·4; $MgCl_2$, 1·7; $CaCl_2$, 1; glucose, 11; Hepes, 21; creatine, 10; taurine, 20; and bovine serum albumin, 0·1 mg/ml, with a pH adjusted to 7·4 with NaOH. This procedure yielded approximately 60% of Ca^{2+}-tolerant cells, which were viable for about 10 h.

Hypertrophic model

Left ventricular hypertrophy was induced in seven animals by the abdominal aortic stenosis technique previously described by Cutilleta, Dowell, Rudnick & Arcille (1975). Briefly, young male rats weighing 180–200 g were anaesthetized by an intramuscular injection of 0·25 ml/g Imalgene 1000 (Rhône Mérieux, France). After opening the abdomen, the suprarenal abdominal aorta was freed from connective tissue and a haemoclip (0·25 mm aperture) was placed around it using Weck forceps. This constriction causes a gradually progressive pressure overload on the left ventricle as the animal grows. Careful postoperative attention was observed after the operation and for the 3 days following surgery an antibiotic therapy (0·1 ml Borgal 7·5% from Distrivet, France) was administered in order to prevent infection. Each operated rat was paired with a sham-operated rat of the same weight and age. The sham-operated rats underwent the same intervention except that no clip was placed on the aorta. Previous work (Aronson & Nordin, 1984) showed that the sham-operated rats are not different from non-operated rats, and as a result they can be considered normal. The animals were fed *ad lib.* and watched over until killed for experiments, 6–7 weeks after surgery. Animals were killed and ventricular cells dissociated as described above. Only hypertrophied hearts in which the heart weight/body weight ratio was over 30% greater than normal heart were selected. This selection criterion explains why our electrophysiological experiments were conducted in only six hypertrophied hearts.

Electrophysiological recordings

Macroscopic current recordings were obtained through the whole-cell voltage clamp method as described by Hamill, Marty, Neher, Sakmann & Sigworth (1981), using a patch clamp amplifier with a 100 MΩ feedback resistance (Headstage CV-4 1/100, Axon Instruments, Foster City, CA, USA). The recording chamber was perfused at a flow rate of about 2 ml/min with the standard superfusion medium. In order to record accurately pure early outward currents, other major overlapping currents had to be blocked. To do this, a sodium-free solution was used as an external solution in order to eliminate the Na^+ current contamination and exclude the possible contribution of either Na^+-activated potassium currents, or of transient currents generated through the Na^+–K^+

pump (Lefevre, Coulombe & Coraboeuf, 1991); in addition, $CoCl_2$ was used to block the slow inward current. As a result, the external solution had the following composition (mM): choline chloride, 135; $MgCl_2$, 1·1; $CaCl_2$, 1·8; $CoCl_2$, 2; mannitol, 0·4; glucose, 10; and Hepes, 10; pH was adjusted to 7·4 with KOH (total K^+ was thus 4–5 mM). The contamination by other potassium currents was minimized by the subtraction analysis of the 4-aminopyridine-sensitive early outward current (I_{to}) before and after applying 3 mM 4-AP (Sigma, France). Because 4-AP is not a totally specific blocker for transient outward current (Kenyon & Gibbons, 1979), the magnitude of I_{to} was measured as a function of membrane potential as the difference between the peak outward current and the current at the end of the pulse. All experiments were performed at room temperature (20–25 °C) in order to slow down the current activation kinetics, and thereby improve voltage control. Patch pipettes, pulled from haematocrit capillaries (o.d. 1·5–1·6 mm), had tip resistances ranging between 1·5 and 2·5 MΩ. The internal solution contained (mM): KCl, 150; $MgCl_2$, 1; EGTA, 5; Hepes, 5; glucose, 10; disodium salt of creatine phosphate, 5; and K_2ATP, 5; pH was adjusted to 7·2 with KOH (EGTA was added to the patch pipette solution to buffer the intracellular Ca^{2+} transient and thus minimize the contribution of the Ca^{2+}-activated currents and the electrogenic Na^+–Ca^{2+} exchange). In whole-cell configuration, the series resistance determined during small voltage steps (±10 mV) from a holding potential of −70 mV was calculated as $R_S = \Delta V_m / I_0$, where R_S is series resistance, ΔV_m is the amplitude of voltage step and I_0 is the maximum capacitive current value. As a result, R_S ranged from 3 to 6 MΩ (mean ± S.D. = 4·84 ± 0·85 MΩ, $n = 76$), equal to 1·5 to 2-fold the pipette resistance. Neither capacitance current nor series resistance with the cell membrane were compensated. As the pipette was in the superfusate, a 5–15 mV junction potential was noted. Therefore all voltage values subsequently obtained were corrected by the value of the junction potential at the pipette tip. Voltage protocol generation, data storage and analysis were performed using a patch amplifier (Axopatch-1 D, Axon Instruments) controlled by a microcomputer (Compaq 386/85 Deskpro) equipped with an appropriate software (pCLAMP, version 5.5.1., Axon Instruments) and interfaced to the amplifier with a 125 kHz Labmaster board.

Statistical methods

All data have been expressed as means ± S.D. in the text, and for sake of clarity as means ± S.E.M. in the graphs. Because the left ventricular free wall cells showed a much higher variability than septal and apex cells (confirmed by the analysis of the variance ratios), no statistical analysis of the I_{to} properties between the topographical groups (left ventricular free wall, septum, apex) were performed. However, statistical significance levels were evaluated for the hypertrophic indices, the morphological and the passive properties of the different groups by using non-parametric tests (Kruskal–Wallis and Mann–Whitney U test), when appropriate. Differences with $P < 0·05$ were considered significant. In spite of the fact that the number of experiments was not equal for each heart among the topographical subgroups, we could check that animal-to-animal variations did not affect comparisons between cells.

RESULTS

Characteristics of I_{to} in normal rats

Passive properties of single ventricular cells

The measurement of morphological and passive electrophysiological properties was performed at the beginning of the experiment in seven control rats. Results are summarized in Table 1. Only rod-shaped and quiescent single cells with well-defined regular cross-striations were chosen while moving the stage of the inverted microscope. Length and width were determined at the greatest span parallel and orthogonal to the long axis of the cells at ×400 magnification. Cellular width and length were not significantly different between the septum, the apex, and the left ventricular free wall groups. However, optically estimated sizes are an approximation which underestimates the surface area by neglecting sarcolemmal infoldings that constitute more than 70% of the total membrane area (Severs, Slade, Powel, Twist & Warren, 1982). Hence, we preferred to refer to membrane capacitance values.

Membrane capacitance was measured in all cells by applying ±10 mV amplitude voltage steps from a −70 mV holding potential and calculated according to the equation:

$$C_m = \tau_c I_0 / \Delta V_m (1 - I_\infty / I_0),$$

where C_m is the membrane capacitance, τ_c is the time constant of the membrane capacitance, I_0 is the maximum capacitive current value, ΔV_m is the amplitude of

TABLE 1. Cell characteristics of normal and hypertrophied ventricles

	Control			Hypertrophied		
	Cell width (μm)	Cell length (μm)	C_m (pF)	Cell width (μm)	Cell length (μm)	C_m (pF)
Septum	17·9±5·8 (n = 12)	81·3±12·3 (n = 12)	177·4±26·1 (n = 12)	26·9±6·6 (n = 16)	79·4±9·4 (n = 16)	277·6±44·4 (n = 16)
Apex	20·5±8·5 (n = 10)	78·3±8·7 (n = 10)	159·8±52·1 (n = 10)	27·5±10·6 (n = 10)	76·5±11·6 (n = 10)	242·7±57·9 (n = 10)
Left free wall	21·0±4·0 (n = 12)	79·0±11·3 (n = 12)	142·6±45·1 (n = 12)	21·7±6·6 (n = 16)	82·7±9·8 (n = 16)	282·7±46·5 (n = 16)

C_m, membrane capacitance. All values are means±S.D.

voltage steps and I_∞ is the amplitude of steady-state current. Whole-cell membrane capacitances were in the range 54–233 pF, similar values to those measured by Scamps *et al.* (1990) or Apkon & Nerbonne (1991). Statistical analysis showed that the regional capacitance values were not significantly different. Accordingly, we concluded that an identical morphometry can be found in the whole ventricular wall.

Zero current potential of single myocytes bathed in normal external solution ranged between −75 to −90 mV. No significant difference was noted between cells isolated from septum, apex and left ventricular free wall (in mV: −83·0±4·2 in septal cells ($n = 12$); −79·4±6·1 in apex cells ($n = 10$); and −80·1±8·4 in left ventricular free-wall cells ($n = 12$).

4-Aminopyridine sensitive early outward currents (I_{to})

Basing our experimental design on the presence of a relatively large early outward current in adult rat cells (Josephson *et al.* 1984) and the topographical heterogeneity of action potentials in isolated rat ventricular myocytes (Watanabe *et al.* 1983), we decided to investigate the amplitude and kinetics of this current in rat ventricular cells from separate groups depending on the anatomical location as defined in the Methods section.

To monitor macroscopic currents, ventricular cells were depolarized from a holding potential (V_h) of −80 mV to voltage tests between −50 to +60 mV in 10 mV increments for 300 ms at an interpulse interval of 5 s (0·2 Hz). The V_h of −80 mV was chosen since it is a membrane potential close to the resting level. Under control conditions (Fig. 1*A*), depolarizing steps to membrane potentials more positive than −30 mV resulted in the appearance of large time- and voltage-dependent transient, or early outward currents which rose rapidly to peak followed by a slower decay to an apparent plateau as described by Josephson *et al.* (1984). To identify the ionic

nature of this early outward current, we conducted our experiments in the presence of 4-AP, a well-known depressing agent of transient potassium currents. The subsequent exposure to 4-AP (Fig. 1*B*) completely abolished the transient outward current peak. However, in most cells, a very slowly decaying time-dependent

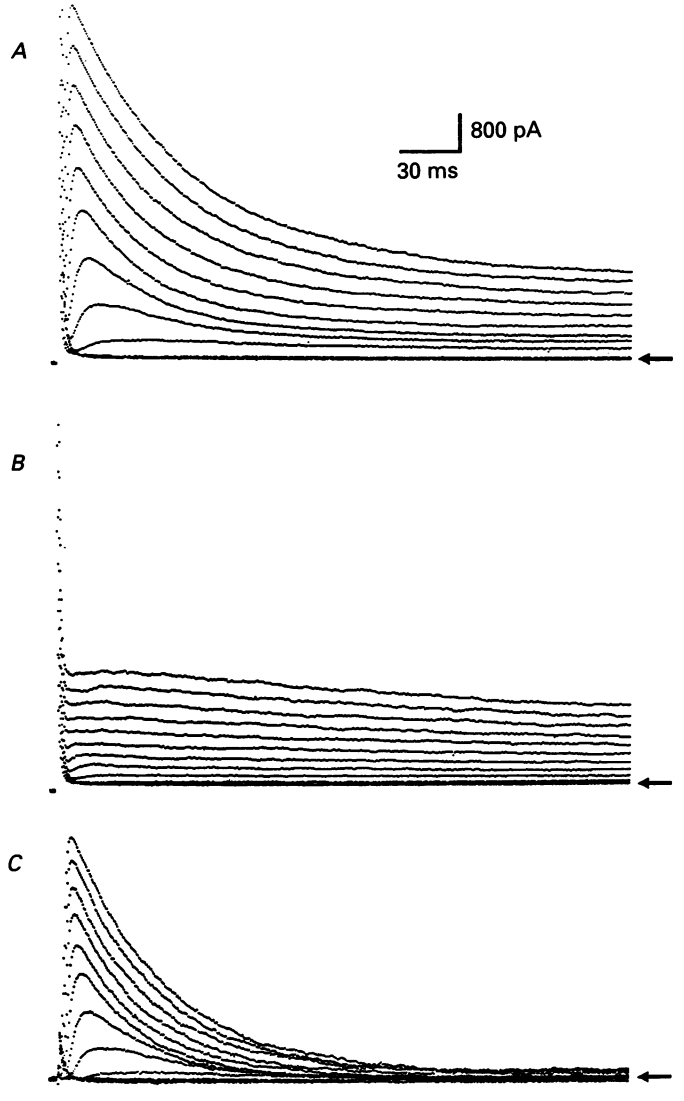

Fig. 1. Pharmacological dissection of the 4-AP-sensitive early outward current (I_{to}) in a normal rat ventricular myocyte. Outward currents were elicited from a holding potential of −80 mV by 300 ms depolarizing voltage-clamp steps (0·2 Hz) delivered in 10 mV increments between −50 and +60 mV (currents were filtered at 10 kHz and digitized at sample intervals of 600 μs). *A*, total currents recorded in control conditions (Na^+-free solution and in presence of 2 mM Co^{2+}); *B*, plateau current traces after 3 min of 3 mM 4-AP superfusion; *C*, 4-AP-sensitive transient currents obtained by subtraction of records in *B* from records in *A*. Arrow indicates zero current level.

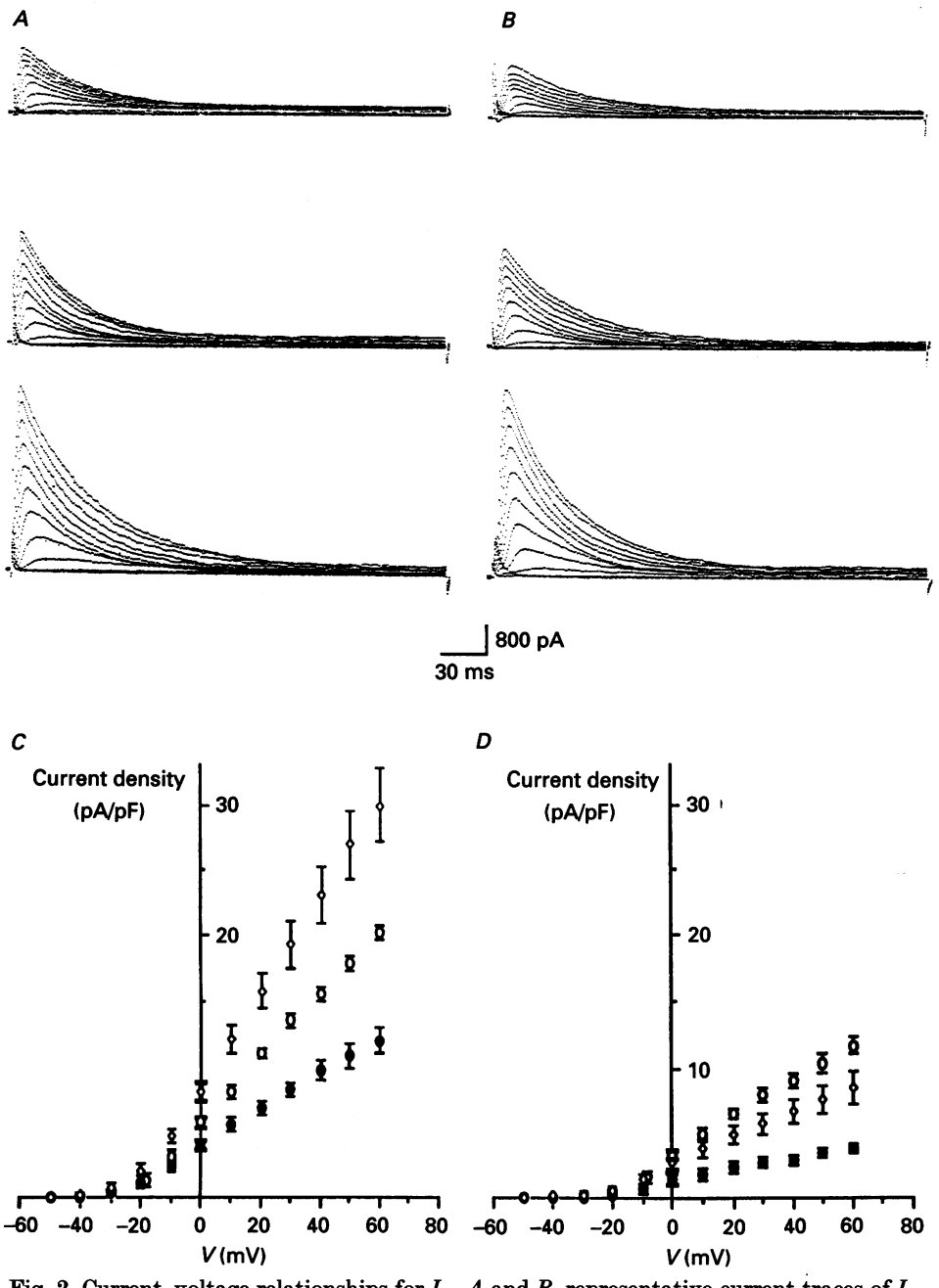

Fig. 2. Current–voltage relationships for I_{to}. *A* and *B*, representative current traces of I_{to} in normal (*A*) and in hypertrophied (*B*) myocytes isolated from septum (top traces), apex (middle traces) and left ventricular free wall (bottom traces). Current traces were obtained by subtraction of records in the presence of 4-AP from those in control conditions induced by 300 ms depolarizing pulses (0·2 Hz) from a holding potential of −80 mV to test voltages ranging from −50 to +60 mV (from lowest to highest traces, in 10 mV increments; currents were filtered at 10 kHz and digitized at sample intervals of 600 μs). *C* and *D*, mean current density–voltage relationships of I_{to}: *C*, in normal

outward current persisted after applying 4-AP. These results are similar to those measured by Apkon & Nerbonne (1991). The effect on the transient peak current which occurred at each membrane potential was achieved in 2–3 min and was fully reversible in 3–4 min. No inward current was elicited during this protocol. The slow inward current which would be expected to develop within this depolarizing step range was totally inhibited in the presence of 2 mM $CoCl_2$. As a result, the elicited early outward current could not be activated by a rise of $[Ca^{2+}]_i$ subsequent to the inflow of calcium current. Indeed, the second component that is known to depend on Ca^{2+} release from the sarcoplasmic reticulum in a number of species (Coraboeuf & Carmeliet, 1982; Escande *et al.* 1987; Giles & Imaizumi, 1988; Hiraoka & Kawano, 1989; Tseng & Hoffman, 1989) was never observed in our experiments. It may be assumed then that this component, if at all present, was inhibited by external $CoCl_2$ and the internal buffer EGTA. Thus, the early outward current that was entirely suppressed by 3 mM 4-AP seemed to be a pure current, although a contribution from a second component cannot be excluded. The subtraction of the total outward currents obtained with 4-AP (Fig. 1*B*) from those obtained without 4-AP (Fig. 1*A*) is represented in Fig. 1*C*.

These findings were consistent with the observations of Josephson *et al.* (1984), Dukes & Morad (1991) and Apkon & Nerbonne (1991) arguing in favour of a single component for the transient outward current in rat ventricular myocytes: its activation was probably independent of changes in $[Ca^{2+}]_i$ and sensitive to the K^+ channel blocker, 4-aminopyridine.

Every analysis thereafter was made on the 4-aminopyridine-sensitive early outward current. Although transient outward currents have been studied in a number of myocardial preparations, there has been no consensus concerning terminology for this current. In this report we refer to the 4-aminopyridine-sensitive early outward current as I_{to} as this term appropriately outlines the rapidly activating and inactivating characteristics of the measured current waveforms as was previously proposed by Apkon & Nerbonne (1991).

Topographical patterns for early outward currents were determined by studying the 4-AP-sensitive currents in the three cell groups. In Fig. 2*A*, we show representative 4-AP-sensitive membrane currents recorded in cells with similar membrane capacitances isolated from the septum, the apex and the left ventricular free wall of normal rats (from top to bottom respectively). There was clear evidence of regional differences in the I_{to} current in the ventricular wall. For depolarizing steps positive to −30 mV, the amplitude of the 4-AP-sensitive outward peak current was strikingly different as a function of cell location in spite of a similar voltage dependence. Currents increased monotonically as a function of the membrane voltage and at first glance the I_{to} in septum appeared smaller than in the apex and smaller in apex than in the left ventricular free wall. In addition to peak amplitude differences, visual inspection of traces suggested that the time course of decay of septum currents was slower than the one of the apex and left ventricular free wall.

---

myocytes isolated from septum (●, $n = 12$), apex (○, $n = 10$) and left ventricular free wall (◇, $n = 12$); *D*, in hypertrophied myocytes isolated from septum (●, $n = 16$), apex (○, $n = 10$) and left ventricular free wall (◇, $n = 16$). Vertical bars represent ± S.E.M.

Our attention was also drawn to regional differences in the dispersion of peak current values. The variability of I_{to} amplitude was indeed very high in the left ventricular free wall group whose heterogeneous population seemed in fact composed of subgroups: two cells with an I_{to} resembling the septum cell current, two cells with a current similar to the apex group current and eight cells exhibiting a much larger I_{to}. It is unlikely that the high variability observed in the free wall group may result from a rat-to-rat variability as it was not found in the other topographical groups (see Methods section).

In order to compare the results obtained among the regional groups on a firmer basis, the magnitude of 4-AP-sensitive outward currents was normalized to membrane capacitance. There is clear evidence from the graph displayed in Fig. 2*C* to show that the I_{to} current density was quite different in septum, apex and left ventricular free wall, whereas the activation threshold for I_{to} current densities was not apparently affected by the topographical origin of cells. I_{to} began to activate between -45 to -25 mV (in mV: $-31{\cdot}7 \pm 6{\cdot}5$ in the septum group ($n = 12$); $-34{\cdot}0 \pm 5{\cdot}7$ in the apex group ($n = 10$); and $-35{\cdot}0 \pm 7{\cdot}4$ in the left ventricular free wall group ($n = 12$)) and went on to increase as voltage steps were made more positive. However, for voltage clamp steps positive to 0 mV, the pattern of I_{to} densities clearly diverged according to the topographical location with the slopes of the current density–voltage relationships assuming the following hierarchical values: left free wall > apex > septum. The average I_{to} current density magnitudes for a +60 mV depolarizing voltage step reached (in pA/pF): $11{\cdot}9 \pm 3{\cdot}3$ in the septum group ($n = 12$); $20{\cdot}2 \pm 1{\cdot}7$ in the apex group ($n = 10$); and $30{\cdot}1 \pm 9{\cdot}2$ in the left free wall group ($n = 12$), with the largest variability obtained in the left ventricular free wall. Since the membrane capacitances did not differ significantly between the groups as mentioned above, it was suggested that there was no obvious link between cellular morphology and I_{to} densities.

These findings indicated that the transient outward current prominent in rat cells is 4-AP sensitive, time and voltage dependent, as previously described by Josephson *et al.* (1984), Dukes & Morad (1991), and Apkon & Nerbonne (1991). In addition, there is a conspicuous influence of the regional distribution on some properties of the 4-AP-sensitive early outward current. These observations led us to compare further the time- and voltage-dependent regional properties of I_{to}.

Voltage dependence of I_{to} kinetics

As suggested by current records visualized in Figs 1 and 2*A*, I_{to} seemed to exhibit inactivation for depolarization steps more positive than -40 mV. In order to assess quantitatively this observation we determined the voltage dependence of steady-state inactivation for I_{to} by applying a 2 s conditioning pulse (at 0·2 Hz) to various membrane voltages followed by a 700 ms test pulse to +40 mV. The prepulse potential was separated from the test pulse by a 3 ms return to V_h to allow a better resolution of current from the variable capacitive current. The magnitude of I_{to} was maximum at a -60 mV prepulse potential and gradually decreased at less negative potentials so that inactivation was complete near membrane potential of +10 mV without unmasking the presence of any inward current. Test currents (I) obtained from the different prepulse potentials were normalized to the maximal elicited

current (I_{max}). Thus, the voltage dependence of I_{to} inactivation could be approximated by a Boltzmann distribution function of the form:

$$I/I_{max} = \{1+\exp[(V_{0.5}-V_c)/k]\}^{-1},$$

where V_c is the voltage of the conditioning pulse, $V_{0.5}$ the potential at which the conductance is half-maximally inactivated and k is the slope factor. Pooled data of steady-state inactivation kinetics from septal cells, apex cells and left ventricular free wall cells were plotted in Fig. 3*A*, *B* and *C* respectively.

The inactivation of I_{to} was a sigmoidal function of membrane potential. Inactivation was almost completely removed at -50 mV and complete inactivation was achieved at potentials between -10 and $+10$ mV. The three inactivation curves were nearly identical, which suggests lack of location-induced modulation in the kinetics of voltage-dependent steady-state inactivation in the three groups. No difference was observed for the mean values in either $V_{0.5}$ (in mV: -35.7 ± 4.7 for septum cells ($n=7$); -36.1 ± 3.8 for apex cells ($n=7$); and -36.0 ± 5.8 for left ventricular free wall cells ($n=6$)), or k (in mV: -5.5 ± 0.5 for septum cells ($n=7$); -5.9 ± 0.6 for apex cells ($n=7$); and -5.9 ± 1.1 for left ventricular free wall cells ($n=6$)).

Therefore, in contrast to the results of Josephson *et al.* (1984), I_{to} as described by Apkon & Nerbonne (1991) did not undergo steady-state inactivation at holding potentials negative to -50 mV; I_{to} inactivation became obvious at more depolarized potentials. This apparent discrepancy could be due to plateau component contributions to steady-state inactivation of the early outward current measured by Josephson *et al.* (1984). Moreover, it may lie in the fact that the voltage dependence of steady-state activation and inactivation parameters is strongly modulated by both extracellular Ca^{2+} and Na^+ (Dukes & Morad, 1991) and by the divalent cations (Agus, Dukes & Morad, 1991). Possibly in our experiments current properties were modified by the use of a divalent cation (cobalt) to block I_{Ca} and the substitution of external Na^+ for a large impermeant cation (choline).

Assuming that the I_{to} current can be kinetically described as the product of inactivation and activation parameters, the voltage dependence of I_{to} steady-state activation was also studied. To do this, chord conductance was determined as a function of membrane potential as previously reported by Lefevre *et al.* (1991):

$$G = I/(V_m - V_{rev}),$$

where G is the chord conductance calculated at membrane potential V_m, I is the current magnitude and V_{rev} is the apparent reversal potential of the current obtained by assuming that I_{to} was a pure potassium current, i.e. that it reversed at the K^+ equilibrium potential (≈ -94 mV in our experiments). As the maximum experimental value of I_{to} did not reflect the maximum chord conductance, we determined the latter using a computer-calculated Boltzmann fit (FIT-Nonlinear Curve Fitting Program for IBM PC) according to the equation:

$$G = G_{max}/\{1+\exp[(V_{0.5}-V_m)/k]\},$$

where G is the chord conductance calculated at membrane potential V_m, G_{max} is the maximum chord conductance, $V_{0.5}$ the potential at which the conductance is half-maximally activated and k is the slope factor describing the steepness of the

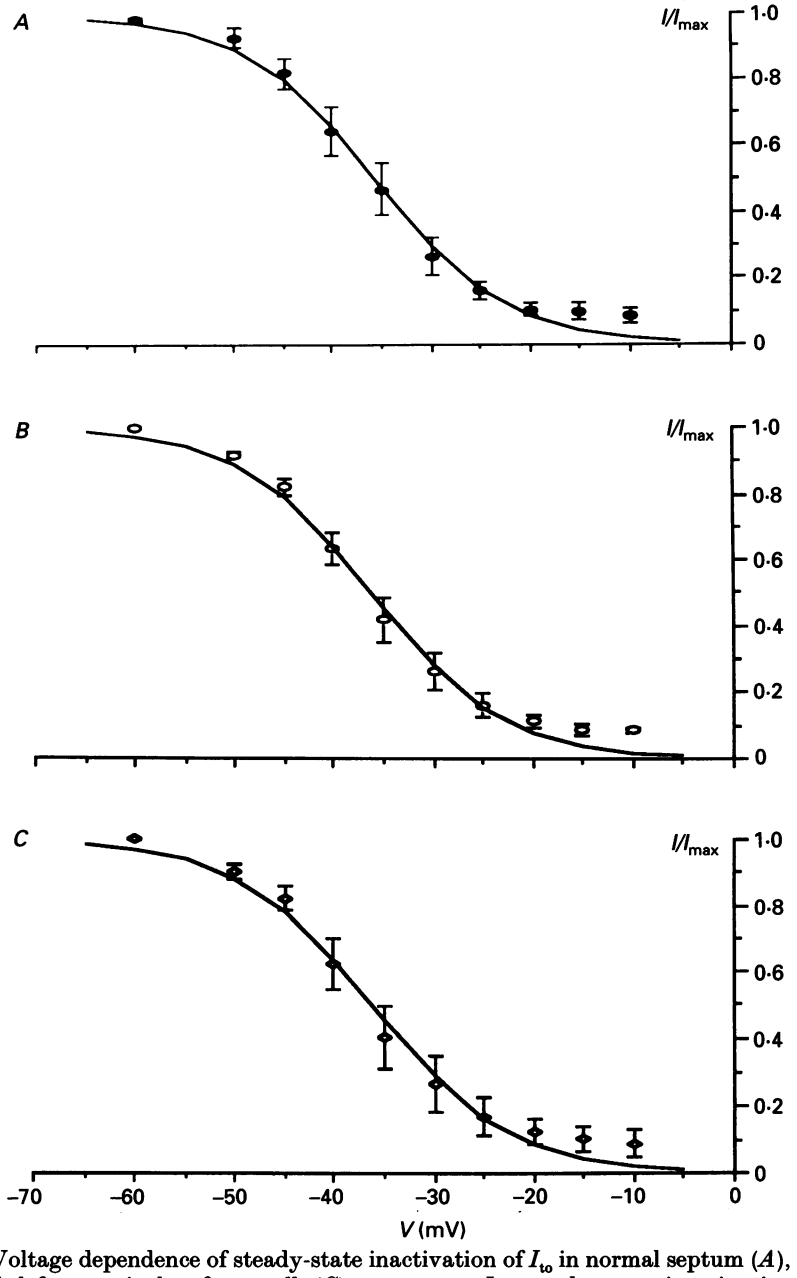

Fig. 3. Voltage dependence of steady-state inactivation of I_{to} in normal septum (*A*), apex (*B*) and left ventricular free wall (*C*) myocytes. I_{to} steady-state inactivation was determined by using a double pulse protocol. Conditioning pulses of 2 s applied from −80 mV to various voltages from −60 to +20 mV (in 10 mV increments) were followed (3 ms delay) by a 700 ms test pulse from −80 to +40 mV. Data were normalized by dividing the test current by the maximal current elicited. The smooth curves were fitted to the mean data points using a Boltzmann distribution as described in text. Vertical bars represent ±S.E.M.

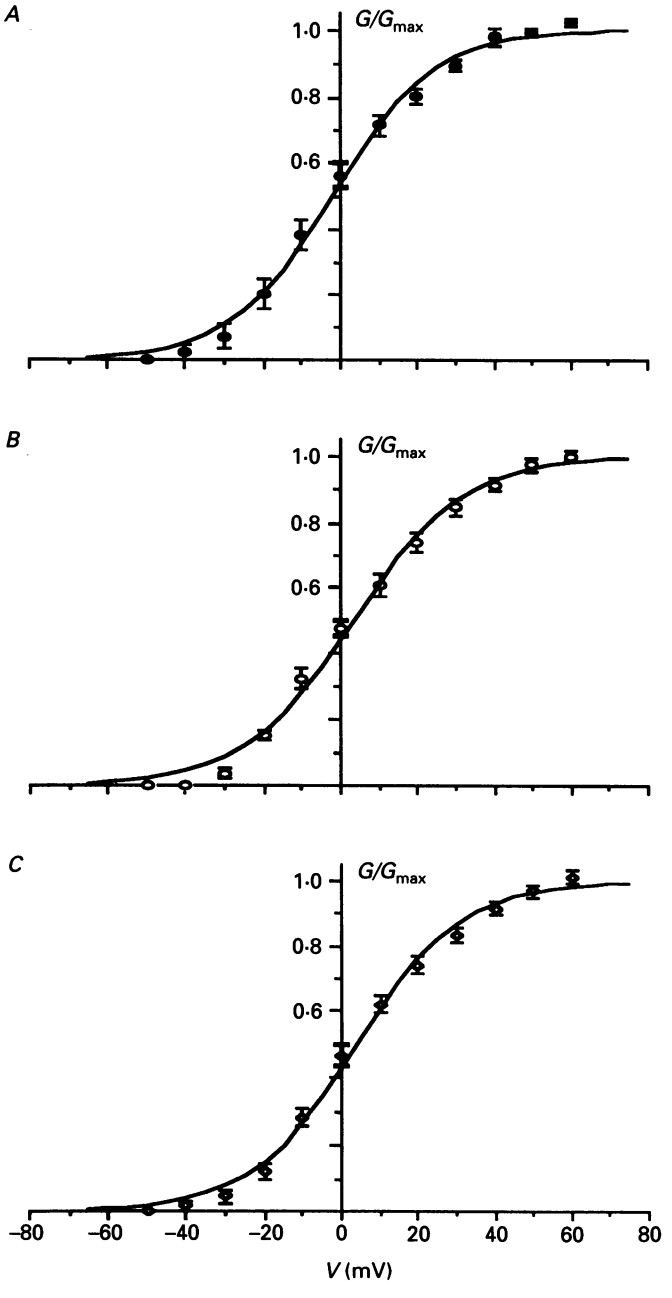

Fig. 4. Steady-state activation–voltage relationships of I_{to} in normal rat ventricular myocytes. Normalized mean chord conductance in septum (*A*), apex (*B*) and left ventricular free wall (*C*) myocytes were plotted *versus* membrane potential. The curves were fitted through the mean data points according to the procedure described in the text. Vertical bars represent ±S.E.M.

activation curve. Using the value of G_{max} obtained through this method, we plotted the normalized whole-cell conductance (G/G_{max}) *versus* the membrane potential.

Partly because V_{rev} is an extrapolated value, the steady-state activation–voltage relationships obtained with this method should be considered as approximations only. Pooled data of steady-state activation kinetics from septal cells, apex cells and left ventricular free wall cells were presented in Fig. 4*A*, *B* and *C* respectively. As demonstrated by the fits to the displayed Boltzmann distribution, the steady-state activation data from the three groups follow nearly identical sigmoidal functions. Hence location-induced modulation was again not observed in the kinetics of voltage-dependent steady-state activation and no significant difference in either $V_{0.5}$ (in mV: $-2{\cdot}4 \pm 8{\cdot}6$ for septum cells ($n = 12$); $3{\cdot}5 \pm 4{\cdot}6$ for apex cells ($n = 9$); and $4{\cdot}1 \pm 5{\cdot}6$ for left ventricular free wall cells ($n = 11$)) or k (in mV: $12{\cdot}3 \pm 3{\cdot}2$ for septum cells ($n = 12$); $12{\cdot}0 \pm 2{\cdot}6$ for apex cells ($n = 9$); and $13{\cdot}8 \pm 4{\cdot}7$ for left ventricular free wall cells ($n = 11$)).

Nevertheless, the G_{max} values calculated as mentioned above were dependent on the considered location. The mean maximal chord conductances normalized to the membrane capacitance were markedly different between groups (in μS/pF): $0{\cdot}08 \pm 0{\cdot}02$ for septum cells ($n = 12$); $0{\cdot}13 \pm 0{\cdot}02$ for apex cells ($n = 9$); and $0{\cdot}18 \pm 0{\cdot}07$ for left ventricular free wall cells ($n = 11$). We noted again in these findings a larger variability in the maximum conductances from the left ventricular wall cells when compared to the other groups. Assuming that the steady-state activation curve may reflect the probability of channel opening for each membrane potential (McDonald, Cavalié, Trautwein & Pelzer, 1986), we can suggest that G_{max} may represent an approximation of the maximal number of channels in the open state. We thus expected that the topographical differences in I_{to} magnitude might be the macroscopic expression of different functional channel densities in the ventricles since we did not observe any statistical difference in membrane capacitances among the topographical groups.

After demonstrating the lack of a differential distribution in steady-state voltage dependence of both I_{to} activation and inactivation, we attempted to define the functional properties of I_{to} by measuring the time courses of activation and inactivation.

Time course of current activation and inactivation

Current traces of Figs 1 and 2*A* show that I_{to} rises rapidly and then declines steadily during maintained depolarization, thus appearing time dependent. The time courses of activation and inactivation were studied by measuring the time to peak and analysing the decay of the 4-AP-sensitive early outward current. Indeed, neither capacitive current nor series resistance with the cell membrane were compensated. However, all current analyses were performed on the 4-AP-sensitive component determined by subtraction of the current recorded in the presence from the one recorded in the absence of 4-AP. Hence we can assume that the possible series resistance errors did not alter our analysis (assuming there are no changes with time, the subtraction procedure enabled elimination of most of the uncompensated capacitive transient, see Fig. 1). This is borne out by other experiments (data not shown) in which the protocols were carried out on the same cell with and without

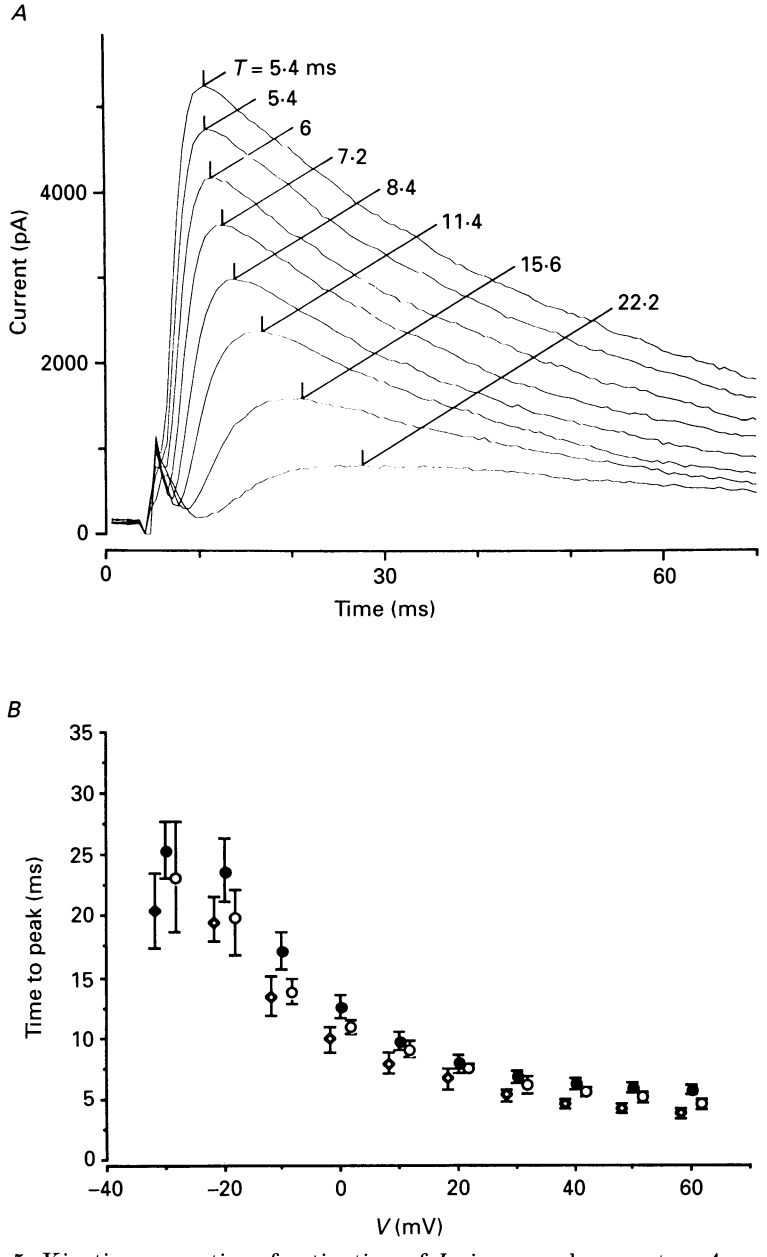

Fig. 5. Kinetics properties of activation of I_{to} in normal myocytes. *A*, representative example of the measurement procedure. 4-AP-sensitive currents were measured at different depolarization voltages (−10 to +60 mV) from a holding potential of −80 mV and time to peak (*T*, in ms) current was determined from the onset of the current rise to the peak current traces. *B*, pooled mean data points of time to peak from septum (●), apex (○) and left ventricular free wall (◇) were plotted *versus* membrane potential. Vertical bars represent ±S.E.M.

series resistance compensation: under these conditions, no appreciable difference in the analysis of 4-AP-sensitive early outward currents is seen.

The presence of an artefact after subtraction in our recording system (Figs 1 and 2*A*) meant a detailed analysis of the activation time course was not possible. However, some direction could be gleaned from the measurement of the times-to-peak current. As shown in Fig. 5*A*, the times to peak were measured from the very beginning of the ascent to the maximum value of the 4-AP-sensitive current traces. At a voltage close to the activation threshold (−30 mV), the I_{to} time to peak was less than 45 ms, and shortened monotonically at more positive voltages (Fig. 5*B*). No appreciable difference in voltage dependence of this I_{to} activation kinetics index was observed between the three topographical groups. Due to methodological problems related to the working temperature (20–25 °C), an overestimation of the physiological times to peak cannot be excluded. However, this voltage dependence of the time-to-peak amplitude has also been measured by Josephson *et al.* (1984) and confirmed by Apkon & Nerbonne (1991) analysing the activation rate constant of the early outward current, calculated from single exponential fits to the rising phases of the currents. Moreover, Apkon & Nerbonne (1991) noted no distinguishable differences in the 4-AP-sensitive component activation rates, from those determined from the total early outward currents.

A change in the kinetics of I_{to} decay may result from an alteration of the K^+ efflux. In order to evaluate this possibility, we analysed the time course of I_{to} inactivation. For depolarizing steps positive to −20 mV, the decay time course was monophasic and using the CLAMPFIT program (Axon Instruments), the best fit ($r \geqslant 0{\cdot}99$) was obtained using a monoexponential model expressed as follows:

$$I_{tot} = A_\tau \exp(-t/\tau) + A_c,$$

where I_{tot} is the total outward current, τ and A_τ are the time constant and the initial amplitude of the phase of inactivation respectively and A_c the amplitude of the time-independent component. Figure 6*A* shows a representative example of fitting current decay time courses obtained for depolarizing pulses stepped to 0 to +60 mV from a V_h of −80 mV. Pooled data of the time constant values obtained with the fitting procedure from septal, apex and left ventricular free wall cells were plotted in Fig. 6*B*. Individual values ranged from 81·1 to 15·7 ms. Within the explored range of membrane potentials (−20 to +60 mV), there was a tendency for the time constants to show a nearly U-shaped relationship as a function of membrane potential. Although the voltage dependence pattern was similar for the three groups, the inactivation time constants for the septum cells were clearly longer than those for the apex and left ventricular free wall cells.

Our findings on inactivation kinetics apparently disagree with some previously reported results (Clark, Giles & Imaizumi, 1988; Hiraoka & Kawano, 1989) on two aspects: (1) we could detect only one component for the I_{to} current decay and (2) there was a tendency to voltage dependence of the inactivation time constants. But these reports dealt with experimental studies performed in rabbit atrial and ventricular cells. Indeed, all the authors working on isolated rat ventricular myocytes (Josephson *et al.* 1984; Dukes & Morad, 1990; Apkon & Nerbonne, 1991) found that inactivation kinetics of transient outward current in this species were best

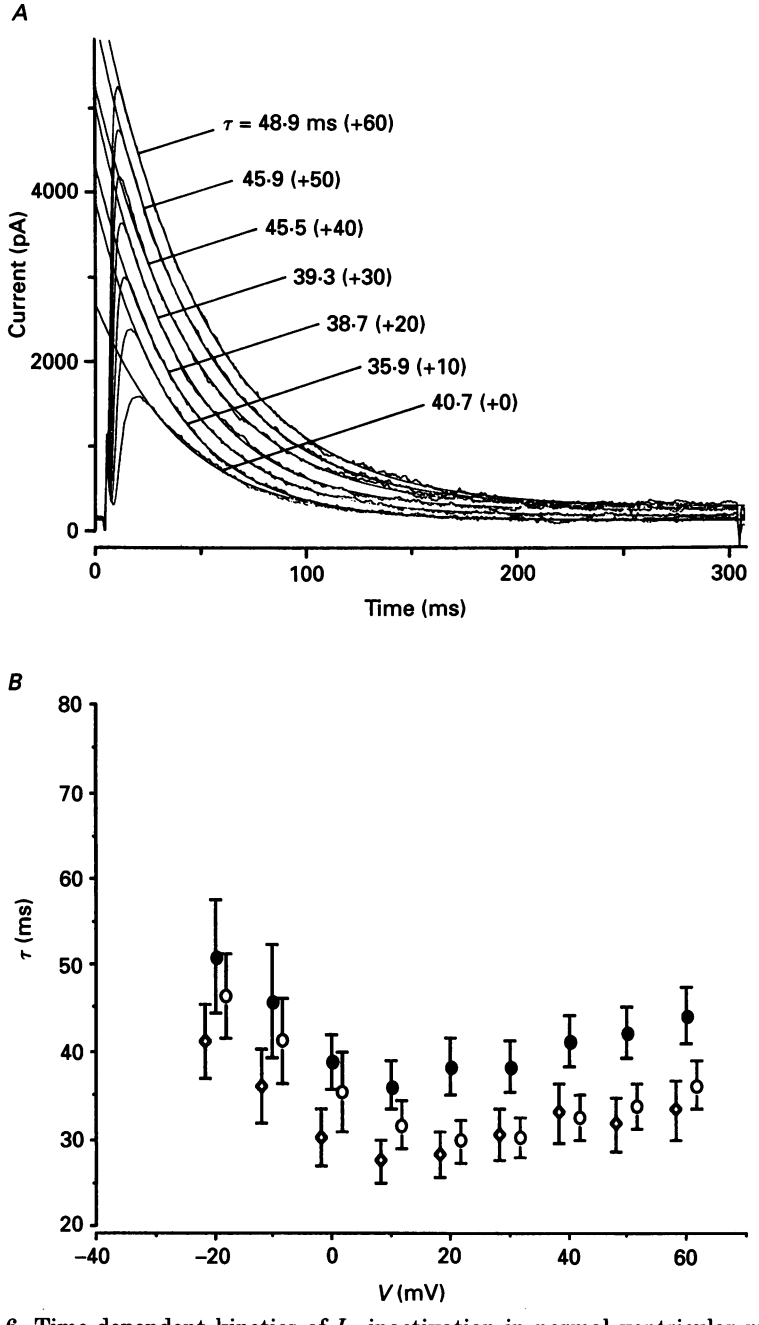

Fig. 6. Time-dependent kinetics of I_{to} inactivation in normal ventricular myocytes. *A*, representative examples of kinetics properties of inactivation of I_{to}. 4-AP-sensitive currents were measured at different depolarizing voltage clamp steps (0 to +60 mV, given in parentheses) from a holding potential of −80 mV. Time constants were obtained by fitting current decays with a computer curve-fitting algorithm (as indicated, in ms). The best fit was obtained with a single exponential model. *B*, mean time constant in normal myocytes isolated from septum (●), apex (○) and left ventricular free wall (◇) plotted *versus* membrane potential. Vertical bars represent ±S.E.M.

fitted by a single exponential function. Nevertheless, they did not detect any voltage dependence for the inactivation time constants. In the absence of a significant criterion (see Methods section), we must stress that we do have some reservation about the voltage dependence of inactivation kinetics suggested from our data. However, it should be noted that one single component for the I_{to} inactivation time course with a similar U-shaped voltage dependence has also been found (Tseng & Hoffman, 1989).

Characteristics of I_{to} in hypertrophy

Morphometry and passive properties

In the experiments conducted with six hypertrophied hearts, the body weight of stenosed rats did not differ from that of normal rats. But as expected with left ventricular hypertrophy, heart weight of stenosed rats was significantly higher than that of normal rats (Table 2). Thus, the heart weight/body weight ratio was significantly greater in the stenosed group than in the normal group, which was our selection criterion for left ventricular hypertrophy.

As regards cellular characteristics (Table 1), the hypertrophied myocytes were wider but as long as the normal ones. However, no morphometric significant difference was noted between the hypertrophic cells isolated from septum, apex and left ventricular free wall. In keeping with the significantly increased cell width, the C_m mean values were significantly higher in hypertrophied myocytes than in normal ones, thus indicating an increased area of electrically chargeable membrane in hypertrophied cells which may be simply attributed to the increase of the apparent surface area. Whole-cell membrane capacitances were in the range of 143–373 pF, similar values to those measured by Scamps *et al.* (1990). The similar increases in both heart weight/body weight ratio and myocyte surface area are in accordance with the expected rate of left ventricular hypertrophy as previously reported by Anversa, Loud, Giacomelli & Wiener (1978). Similarly in morphometric measurements, there were no significant topographical differences for C_m. The mean resting potential values for each topographical group were not significantly different either (in mV: $-81{\cdot}3 \pm 4{\cdot}9$ for septum cells ($n = 16$); $-81{\cdot}6 \pm 3{\cdot}4$ for apex cells ($n = 10$); and $-79{\cdot}2 \pm 3{\cdot}6$ for left ventricular free wall cells ($n = 16$)).

I_{to} in hypertrophied myocytes

In the previous section, we demonstrated a differential distribution of I_{to} in single myocytes isolated from the septum, the apex and the left ventricular free wall from normal rat hearts. Notwithstanding its unequal magnitude, I_{to} was present in all the studied cells. Then in an attempt to explore more deeply the apparent lack of transient outward currents in human ventricular myocytes from hypertrophied hearts (Bénitah *et al.* 1992*a*), we undertook a thorough study of the effects of myocardium hypertrophy on I_{to} in rat hearts.

In these series of voltage clamp experiments, the same protocols and analyses as in normal myocytes were carried out. The average magnitude of I_{to} appeared only slightly smaller in hypertrophied cells (Fig. 2*B*) than in normal cells (Fig. 2*A*). In the same way as in the normal group, there was a considerable cell-to-cell variation in I_{to} magnitude from the hypertrophied left ventricular free wall. In fact, ten cells showed

I_{to} characteristics close to those of apex cells and the six remaining ones showed I_{to} characteristics close to those of septal cells. As a result in hypertrophied cells, the topographical pattern of mean I_{to} magnitude values was: apex > left ventricular free wall > septum. Again, the large difference within-group variances precluded us from comparing the three topographical groups.

TABLE 2. Characteristics of control and hypertrophied rats

Rats	Body weight (g)	Heart weight (g)	Heart wt/body wt (mg/g)
Normal	427·7 ± 36·5 ($n = 7$)	1·6 ± 0·2 ($n = 7$)	3·7 ± 0·3 ($n = 7$)
Hypertrophied	442·7 ± 35·1 ($n = 6$)	2·4 ± 0·3 ($n = 6$)	5·5 ± 0·6 ($n = 6$)

All values are means ± S.D.

The mean current density–voltage relationships are shown in Fig. 2*D*, representing averaged data from sixteen septum, ten apex and sixteen left ventricular free wall hypertrophied myocytes. These findings clearly show that I_{to} density was smaller in hypertrophied than in normal myocytes for the whole range of studied membrane voltages and for each of the considered groups. The slopes of current density–voltage relationships were much less steep and I_{to} activation threshold was shifted to potentials more positive than in the normal groups. The differences in I_{to} regional distribution between groups persisted, although they tended to decrease as compared to the normal groups. The mean current threshold was (in mV): $-26·9 \pm 6·5$ in the septum group ($n = 16$); $-27·5 \pm 10·6$ in the apex group ($n = 10$); and $-21·7 \pm 6·5$ in the left free wall group ($n = 16$); values did not differ greatly from each other, but shifted to more positive potentials when compared with normal groups. The average I_{to} current density magnitudes for a +60 mV depolarizing voltage step attained (in pA/pF): $3·8 \pm 1·5$ in the septum group ($n = 16$); $11·6 \pm 2·0$ in the apex group ($n = 10$); and $8·4 \pm 5·0$ in the left free wall group ($n = 16$) (with the largest variability recorded in the left ventricular free wall). Thus in the same way as with normal cells, we hypothesized that the smaller 4-AP-sensitive early outward currents found in hypertrophied cells might reflect a reduced channel density and other differences in channel current properties: these possibilities are discussed below.

The steady-state inactivation curves were determined in seven septum, eight apex and ten left ventricular free wall cells from hypertrophied hearts (Fig. 7*A*, *B* and *C* respectively). Fitting the average data obtained from those myocytes to a Boltzmann distribution function gave the half-inactivation points at $-33·7 \pm 3·5$, $-34·5 \pm 2·5$, and $-31·2 \pm 6·5$ mV (for the septum, apex and left ventricular free wall groups respectively) and a slope factor of $-6·3 \pm 1·3$, $-5·3 \pm 1·0$ and $-5·4 \pm 1·1$ mV (for the septum, apex and left ventricular free wall groups respectively). As with normal groups, neither $V_{0·5}$ nor k differed significantly between the different locations. Furthermore, no significant difference was observed between normal and hypertrophied myocytes (Figs 3 and 7). Thus there was no hypertrophy-induced change in the availability of the channel for opening in hypertrophied myocytes.

The I_{to} steady-state activation–voltage relationships in hypertrophied cells resembled those of normal cells with a similar sigmoidal dependence on membrane potential. The averaged activation parameter data are plotted in Fig. 8*A*, *B* and *C* (for the septum, apex and left ventricular free wall groups respectively): the

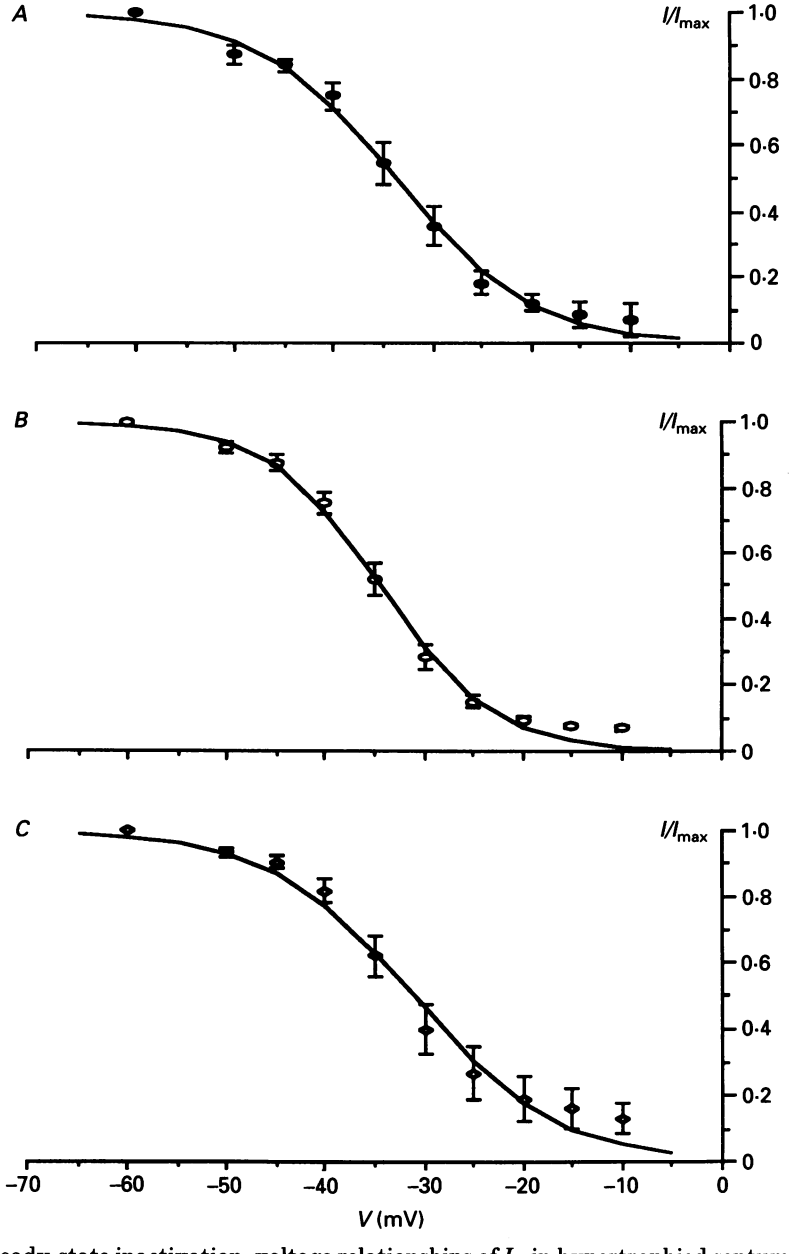

Fig. 7. Steady-state inactivation–voltage relationships of I_{to} in hypertrophied septum (*A*), apex (*B*) and left ventricular free wall (*C*) myocytes. The smooth curves were fitted to the mean data points using a Boltzmann distribution as described in text. Vertical bars represent ±S.E.M.

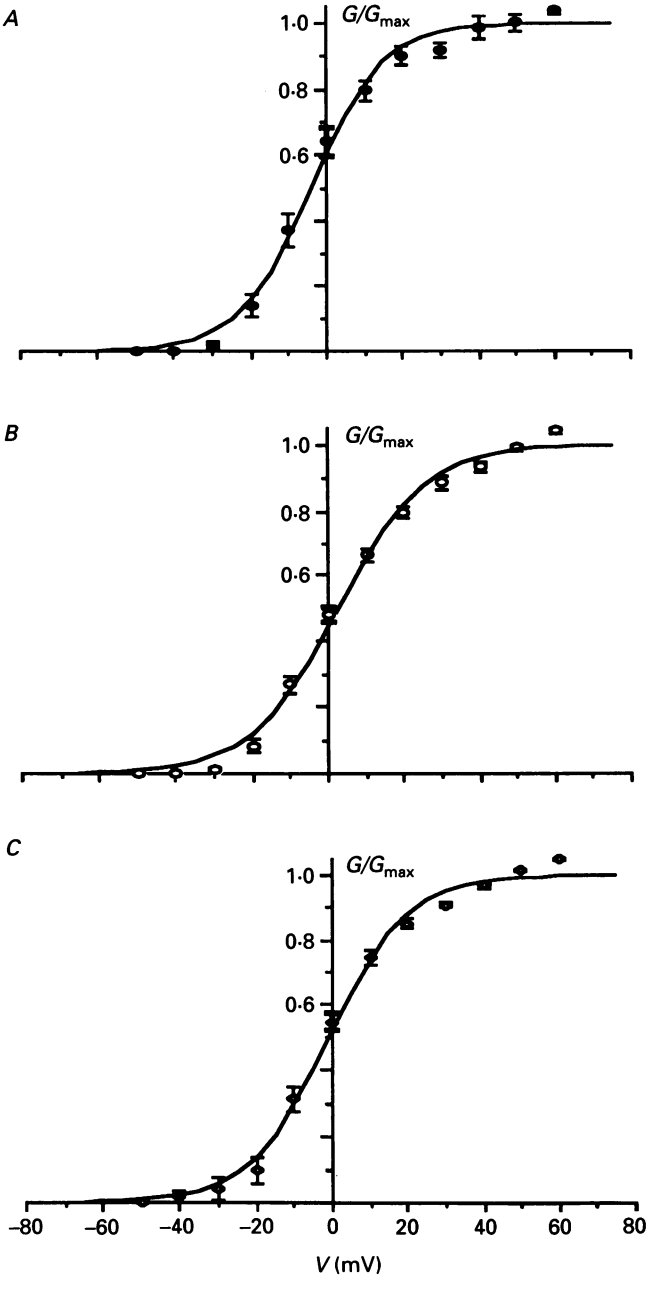

Fig. 8. Steady-state activation–voltage relationships of I_{to} in hypertrophied rat ventricular myocytes. Normalized mean chord conductance in septum (*A*), apex (*B*) and left ventricular free wall (*C*) myocytes were plotted *versus* membrane potential. The curves were fitted through the mean data points according to the procedure described in the text. Vertical bars represent ±S.E.M.

normalized data points for the three topographical groups were fitted by Boltzmann distribution functions. With respect to the location, mean $V_{0.5}$ was (in mV) -3.7 ± 7.5 in septum cells ($n = 15$), 2.5 ± 3.5 in apex cells ($n = 9$) and -1.6 ± 7.2 in left ventricular free wall cells ($n = 15$); the corresponding values for k were 8.7 ± 2.6, 11.3 ± 1.5 and 10.0 ± 2.2 respectively. As with normal hearts, the activation parameters did not show any difference between the topographical groups (Figs 4 and 8). However, it could be observed that k seemed smaller in the hypertrophied groups than in the normal groups. This observation was consistent with the current threshold shift to more positive potentials, while the maximum I_{to} magnitude did not change.

As with normal groups, the mean maximal chord conductances normalized to the membrane capacitance were different in hypertrophied groups (in μS/pF): 0.02 ± 0.01 for septum cells ($n = 15$); 0.07 ± 0.01 for apex cells ($n = 9$); and 0.05 ± 0.03 for left ventricular free wall cells ($n = 15$). But in both normal and hypertrophied cells, the observed patterns might reflect differences in C_m, i.e. in membrane area. We therefore compared the mean maximal chord conductances before normalizing to membrane capacitance. Using this procedure, we no longer observed normal *versus* hypertrophy differences except for the septal region: 6.7 ± 2.9 *versus* 13.8 ± 4.5 μS for septum cells, 17.9 ± 6.8 *versus* 18.6 ± 7.8 μS for apex cells and 15.8 ± 10.5 *versus* 26.0 ± 13.0 μS for left ventricular free wall cells (in hypertrophy *versus* normal respectively). Assuming G_{max} was correlated with the number of functional channels as mentioned above, we consequently considered that there was a strong likelihood of differences in the functional channel densities in hypertrophied *versus* normal hearts for both the apex and left ventricular free wall regions, but not in the number of functional channels. However, this hypothetical picture could not apply to the septal region in which we have to assume an absolute hypertrophy-induced decrease in the number of functional channels. A speculative explanation may be based on the fact that hypertrophy would be unable to induce I_{to} channel neosynthesis (in the opposite way to the one proposed by Scamps *et al.* (1991) regarding the adaptational changes of $I_{Ca,L}$ during the hypertrophic process in rat hearts). Furthermore, I_{to} channels in hypertrophied cells may be influenced by a modified environment thus altering their kinetic behaviour (a similar situation may occur for septal I_{to} channels in normal cells).

As shown in Fig. 2*B*, the rises of current traces from hypertrophied cells were slowed down as compared to those recorded in a normal cell (Fig. 2*A*). This observation was borne out by the plot of mean times-to-peak data obtained within the range of explored membrane potentials in hypertrophied cells (Fig. 9*A*). No difference between location groups among hypertrophied cells was noted, but there was a marked lengthening of activation in hypertrophied cells compared to the normal ones (Figs 5 and 9) for the whole range of explored voltages.

Figure 9*B* illustrates another major difference between hypertrophied and normal cells for the mean values of I_{to} inactivation time constants. Compare Figs 6 and 9*B*; there is clear evidence that the time course of I_{to} inactivation was different in hypertrophied myocytes than in the normal ones. If the general pattern of inactivation time constants–voltage relationships was similar in both groups (absence of regional differences), the whole kinetics were markedly slowed down in

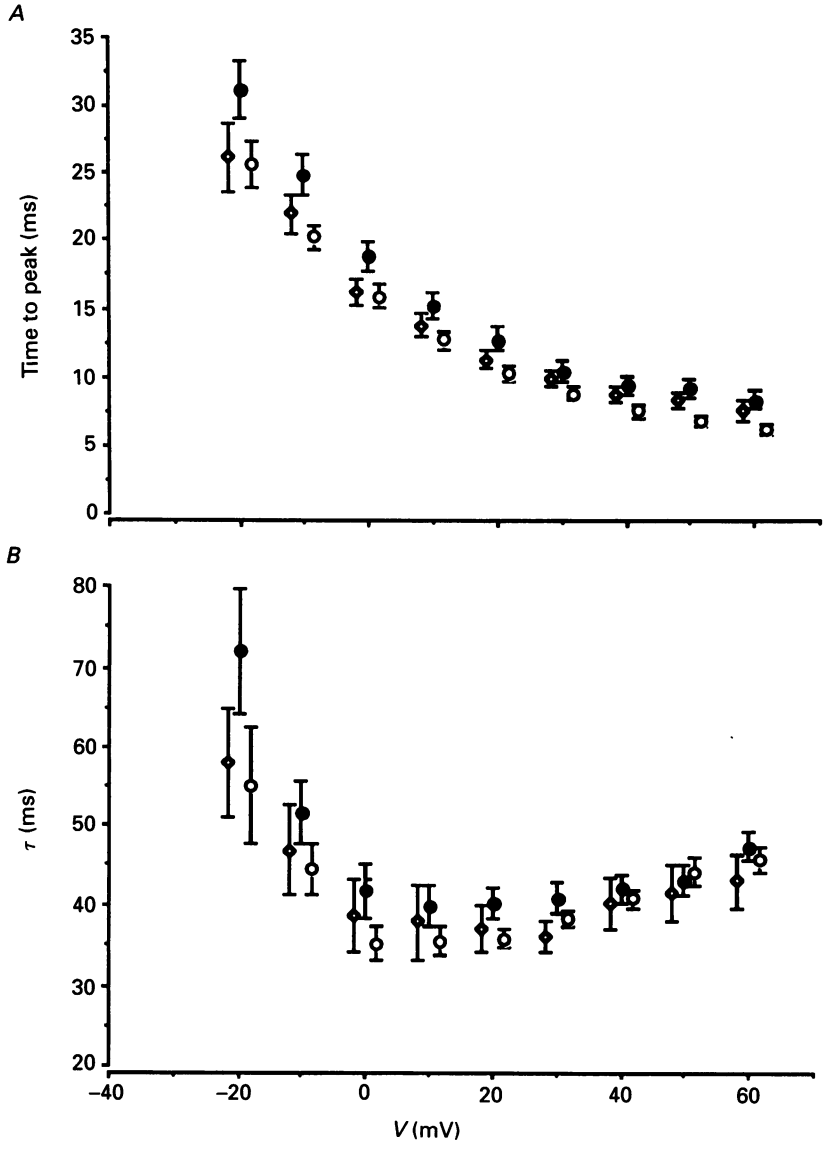

Fig. 9. Comparison of kinetics properties of I_{to} in hypertrophied myocytes isolated from septum (●), apex (○) and left ventricular free wall (◇). *A*, times to peak were plotted *versus* membrane potential. *B*, pooled mean data of inactivation time constants obtained by curve-fitting algorithm were plotted *versus* membrane potential. Vertical bars represent ±S.E.M.

hypertrophied groups. As a result, the time constants of current decay seemed to undergo a homogenizing trend towards the level of values found in both normal and hypertrophied septum cells. The mean time constants measured at depolarizing steps of +40 mV were: 42·1±6·8 *versus* 41·2±9·7 ms for septum cells; 40·8±4·0 *versus* 32·5±8·3 ms for apex cells; and 42·1±6·8 *versus* 32·9±11·8 ms for the left ventricular free wall cells (in hypertrophy *versus* normal cells respectively).

DISCUSSION

The major findings of this paper are threefold. (1) On the basis of our topographical model, there is clear evidence of a differential distribution of I_{to} in septum, apex and left ventricular free wall myocytes from normal rat hearts. (2) This physiological topographical heterogeneity of I_{to} tends to decrease in the abdominal aortic stenosis-induced left ventricular hypertrophy through a global reduction of the current density. (3) The lower variability of currents in septum and apex groups compared to the left ventricular free wall group in both normal and hypertrophied cells lends support to the assumption that a differential distribution of I_{to} may exist not only with reference to an epicardial–endocardial spectrum but also with respect to the anatomical considered regions.

Regional variation of I_{to} in normal rat hearts

Our findings demonstrated differences in the density of 4-AP-sensitive early outward current in the septum, the apex and the left ventricular free wall of the rat heart. The mean current density in apex cells was clearly about twice as high as in septum cells and the mean current density of left ventricular free wall cells was about three times higher than in septum cells as shown in Fig. 2*C*. To our knowledge, no such differential distribution of I_{to} has been reported so far. Yet this distribution was consistent, to a certain extent, with the previous findings of Watanabe *et al.* (1983) who reported the fact that action potentials recorded from the apical region were shorter than those from the base of the left ventricle.

We found that the variability of I_{to} is much higher in the left ventricular free wall group than in both other groups and that such variability apparently resulted from a rather heterogeneous composition of this group (see Results). Indeed, a large variability for the transient outward current was previously reported in rabbit ventricle studies (Giles & Imaizumi, 1988), and as suggested by these authors, we could not rule out the possibility that cell-to-cell differences in I_{to} size in left ventricular free wall were due to real differences in its distribution between epicardium and endocardium in the rat heart. The assumption of a regional difference in action potential morphology between epicardium and endocardium, probably related to a differential distribution of transient outward currents, was supported by canine ventricular tissue studies (Litovsky & Antzelevitch, 1988). A 'spike and dome' configuration was recorded in epicardial preparations but was absent in endocardium. Responses to different stimulation protocols and pharmacological interventions led to the proposal of the virtual absence of a transient outward K^+ current in endocardium as opposed to epicardium in this model. The correlation of the presence of a notch in the epicardial action potential and a prominent transient outward current (I_{to1}) in isolated epicardial myocytes was recently ascertained by Furukawa *et al.* (1990) in cat hearts; the opposite pattern was uncovered in subendocardial layers. In an attempt to describe the differential regional distribution of the 4-AP-sensitive outward currents (I_t) in rabbit left ventricles, a similar procedure analysing epicardial and endocardial layers separately has recently been reported by Fedida & Giles (1991).

Differences in the resting potential might alter the availability and the recovery of

the early outward current and thus induce apparent regional differences in the current characteristics. In fact, no differences for the zero current potential were recorded between the three groups. The differential distribution of I_{to} densities observed in normal rat ventricles could not be correlated to relative shifts of steady-state activation and inactivation curves since there were no significant differences in half-activation and inactivation voltages, nor in slope factors between groups. There was only a slight non-significant tendency for the mean inactivation time constants of normal septum cells to assume higher values than those of both other groups within the +20 to +60 mV range (Fig. 6). Accordingly no consistent explanation for the regional variations in I_{to} densities could be deduced from the steady-state activation and inactivation kinetics, nor were the different regional time courses of current decay of any significant value. Since no single channel studies were actually performed in this work, we could not exclude the existence of regional differences in the properties of the single transient outward current channels, though we should like to consider the following assumptions: (1) the channel opening probability is related to the voltage-dependent macroscopic current as suggested by McDonald *et al.* (1986) for the Ca^{2+} channel current and probably also for the transient outward current channels as proposed by Clark *et al.* (1988) on the basis of similar effects of stimulus frequency on the whole-cell amplitude and the mean open probability of the channel; (2) the current–voltage relationship and slope conductances for single channels may be similar from one region to another. Provided that these assumptions are correct, then the computed maximal conductance, G_{max}, for septum, apex and left ventricular free wall cells may be viewed as an indirect estimate of the maximal number of channels in the open state. Continuing thus, it may be expected that the density of I_{to} functional channels is reduced in septal cells when compared to the apex and left ventricular free wall cells in normal rat hearts. A similar conclusion was recently drawn from single channel studies performed in rabbit left ventricles by Fedida & Giles (1991): single I_t channels in rabbit endocardium and epicardium had the same amplitude and kinetics, whereas current density was higher in epicardial cells than in endocardial or papillary muscle cells. Moreover, the present findings on hypertrophied rat heart seemed to agree with our assumption on a differential distribution of functional channel densities.

Distribution pattern of I_{to} in hypertrophied rat hearts

Regional differences in the electrophysiological properties of the ventricular tissue of the heart were first outlined by Keung & Aronson (1981). Working on endocardial, epicardial and papillary muscle fibres obtained from hypertrophied and normal hearts, these authors showed that hypertrophy induced by renal hypertension may be a non-uniform process that affects the ventricular wall layers to a different degree.

Direct evidence for a global decrease in I_{to} current density in the hypertrophied rat ventricle results from our experiments. As mentioned above, it should be stressed that this decrease was related to a consistent reduction in maximal I_{to} conductances normalized to membrane capacitances. No hypertrophy-induced changes of the steady-state activation and inactivation parameters were involved in this process. One plausible explanation might lie in the absence of I_{to} channel neosynthesis during the hypertrophic process leading to a decrease of channel density per surface area

unit, but not of the absolute number of channels per cell, at least in the apex and free wall regions. Such behaviour might be the reverse of the adaptational process of Ca^{2+} channels to pressure overload in which the total number of Ca^{2+} channels was increased while Ca^{2+} channel density was maintained in hypertrophied rat ventricular cells (Mayoux, Callens, Swynghedauw & Charlemagne, 1988); conversely, it may be comparable to the time course pattern of other membrane proteins whose decreased density during cardiac overload suggests a non-regulation for the genes coding for these receptors (Mansier *et al.* 1990). Moreover, it should be mentioned that the decrease of I_{to} current density observed in hypertrophied cells was of the same order as that observed during the early stages of development in rat ventricular myocytes (Kilborn & Fedida, 1990), even though further investigations would be mandatory to elucidate and compare the molecular mechanisms for both these processes.

As shown in normal hearts, the differential distribution among the studied regions persisted although it tended to decrease. Regarding time kinetics, we noted a global lengthening of times to peak in all regions and a particular pattern change of inactivation kinetics; time constants of current decay were not prolonged in hypertrophied septal cells whereas they were markedly lengthened in apex and left free wall regions, resulting in a homogenization of values in all the considered regions. Thus the hypertrophy-induced inactivation kinetics changes associated with the global reduction of I_{to} densities in different regions of the left ventricle may suggest a homogenizing process related to pressure overload-dependent structural and functional alterations. Furthermore, assuming regional differences in the absolute number of functional channels and an absence of channel neosynthesis during the hypertrophic process, we may expect the appearance of environmental changes of channels within the membrane which should be able to modulate time-dependent kinetics without altering both activation and inactivation parameters.

We have demonstrated in a previous study (Bénitah *et al.* 1992*a*) that the calcium channel current is largely dominant as compared to transient outward currents in human septal cells from ventricular hypertrophy subsequent to chronic pressure overload. From our experimental data we expect that two factors can underlie this ionic pattern in the human heart; (1) the septum may be a region in which the transient outward current is not originally prominent, and (2) the hypertrophic process is clearly a potent contributing factor to reducing this current.

We thank Dr M. Delmar for his helpful information and critical reading of the manuscript, and B. Calime for secretarial assistance. This work was supported by a grant-in-aid from the Groupe de Réflexion sur la Recherche Cardiovasculaire, the laboratoires Squibb (France), and Actions intégrées Franco–Espagnol (92040).

REFERENCES

Agus, Z. S., Dukes, I. A. & Morad, M. (1991). Divalent cations modulate the transient outward current in rat ventricular myocytes. *American Journal of Physiology* **261**, C310–318.

Antzelevitch, C., Sicouri, S., Litovsky, S. H., Lukas, A., Krishnan, S. C., Di Diego, J. M., Gintant, G. A. & Liu, D. W. (1991). Heterogeneity within the ventricular wall. Electrophysiology and pharmacology of epicardial, endocardial, and M cells. *Circulation Research* **69**, 1427–1449.

ANVERSA, P., LOUD, A. V., GIACOMELLI, F. & WIENER, J. (1978). Absolute morphometric study of myocardial hypertrophy in experimental hypertension. *Laboratory Investigation* **38**, 597–605.

APKON, M. & NERBONNE, J. M. (1991). Characterization of two distinct depolarization-activated K^+ currents in isolated adult rat ventricular myocytes. *Journal of General Physiology* **97**, 973–1011.

ARONSON, R. S. & NORDIN, C. (1984). Electrophysiological properties of hypertrophied myocytes isolated from rats with renal hypertension. *European Heart Journal* **5**, suppl. F, 339–345.

BÉNITAH, J.-P., BAILLY, P., D'AGROSA, M.-C., DA PONTE, J.-P., DELGADO, C. & LORENTE, P. (1992*a*). Slow inward current in single cells isolated from adult human ventricles. *Pflügers Archiv* **421**, 176–187.

BÉNITAH, J.-P., DELGADO, C., GOMEZ, A. M., BAILLY, P., DA PONTE, J.-P. & LORENTE, P. (1992*b*). Characteristics of the transient outward current within the ventricular wall in normal and hypertrophied rat ventricles. XIVth Congress of the European Society of Cardiology, August 1992, Barcelona, Spain. *European Heart Journal* **13**, 397 (abstract 2313).

CLARK, R. B., GILES, W. R. & IMAIZUMI, Y. (1988). Properties of the transient outward current in rabbit atrial cells. *Journal of Physiology* **405**, 147–168.

CORABOEUF, E. & CARMELIET, E. (1982). Existence of two transient outward currents in sheep cardiac Purkinje fibers. *Pflügers Archiv* **392**, 352–359.

CUTILLETA, A. F., DOWELL, T., RUDNICK, M. & ARCILLE, R. A. (1975). Regression of myocardial hypertrophy. I. Experimental model changes in heart weight nucleic acids and collagen. *Journal of Molecular and Cellular Cardiology* **7**, 767–781.

DECK, K. A. & TRAUTWEIN, W. (1964). Ionic currents in cardiac excitation. *Pflügers Archiv* **280**, 63–80.

DUKES, I. A. & MORAD, M. (1991). The transient K^+ current in rat ventricular myocytes: evaluation of its Ca^{2+} and Na^+ dependence. *Journal of Physiology* **435**, 395–420.

ESCANDE, D., COULOMBE, A., FAIVRE, J. F., DEROUBAIX, E. & CORABOEUF, E. (1987). Two types of transient outward currents in adult human atrial cells. *American Journal of Physiology* **252**, H142–148.

ESCANDE, D., LOISANCE, D., PLANCHE, C. & CORABOEUF, E. (1985). Age-related changes of action potential plateau shape in isolated human atrial fibers. *American Journal of Physiology* **249**, H843–850.

FEDIDA, D. & GILES, W. R. (1991). Regional variations in the action potentials and transient outward current in myocytes isolated from rabbit left ventricle. *Journal of Physiology* **442**, 191–209.

FOZZARD, H. A. & HIRAOKA, M. (1973). The positive dynamic current and its inactivation properties in cardiac Purkinje fibres. *Journal of Physiology* **234**, 569–586.

FURUKAWA, T., MYERBURG, R. J., FURUKAWA, N., BASSETT, A. L. & KIMURA, S. (1990). Differences in transient outward currents of feline endocardial and epicardial myocytes. *Circulation Research* **67**, 1287–1291.

GILES, W. R. & IMAIZUMI, Y. (1988). Comparison of potassium currents in rabbit atrial and ventricular cells. *Journal of Physiology* **405**, 123–145.

GINTANT, G. A., COHEN, I. S., DATYNER, N. B. & KLINE, R. P. (1991). Time-dependent outward currents in the heart. Transient outward current in cardiac fibers. In *The Heart and Cardiovascular System*, ed. FOZZARD, H. A., HABER, E., JENNINGS, R. G., KATZ, A. M. & MORGAN, H. E., pp. 1138–1156. Raven Press, New York.

HAMILL, O. P., MARTY, A., NEHER, E., SAKMANN, B. & SIGWORTH, F. J. (1981). Improved patch clamp technique for high-resolution current recording from cells and cell-free membrane patches. *Pflügers Archiv* **391**, 85–100.

HIRAOKA, M. & KAWANO, S. (1989). Calcium-sensitive and insensitive transient outward current in rabbit ventricular myocytes. *Journal of Physiology* **410**, 187–212.

JOSEPHSON, I. R., SANCHEZ-CHAPULA, J. & BROWN, A. M. (1984). Early outward current in rat single ventricular cells. *Circulation Research* **54**, 157–162.

KENYON, J. L. & GIBBONS, W. R. (1979). 4-Aminopyridine and the early outward current of sheep cardiac Purkinje fibers. *Journal of General Physiology* **73**, 139–157.

KEUNG, E. C. (1989). Calcium current is increased in isolated adult myocytes from hypertrophied rat myocardium. *Circulation Research* **64**, 753–763.

KEUNG, E. C. & ARONSON, R. S. (1981). Non-uniform electrophysiological properties and electrotonic interaction in hypertrophied rat myocardium. *Circulation Research* **49**, 150–158.

KILBORN, M. J. & FEDIDA, D. (1990). A study of the developmental changes in outward currents of rat ventricular myocytes. *Journal of Physiology* **430**, 37–60.

KLEIMAN, R. B. & HOUSER, S. R. (1988). Calcium currents in normal and hypertrophied isolated feline ventricular myocytes. *American Journal of Physiology* **255**, H1434–1442.

LEFEVRE, I. A., COULOMBE, A. & CORABOEUF, E. (1991). The calcium antagonist D600 inhibits calcium-independent transient outward current in isolated rat ventricular myocytes. *Journal of Physiology* **432**, 65–80.

LITOVSKY, S. H. & ANTZELEVITCH, C. (1988). Transient outward current prominent in canine ventricular epicardium but not endocardium. *Circulation Research* **62**, 116–126.

MCDONALD, T. F., CAVALIÉ, A., TRAUTWEIN, W. & PELZER, D. (1986). Voltage-dependent properties of macroscopic and elementary calcium channel currents in guinea pig ventricular myocytes. *Pflügers Archiv* **406**, 437–448.

MANSIER, P., CHEVALIER, B., MAYOUX, E., CHARLEMAGNE, D., OLLIVIER, L., CALLENS, F. & SWYNGHEDAUW, B. (1990). Membrane proteins of the myocytes in cardiac overload. *British Journal of Clinical Pharmacology* **30**, 43–48S.

MAYOUX, E., CALLENS, F., SWYNGHEDAUW, B. & CHARLEMAGNE, D. (1988). Adaptational process of the cardiac Ca^{2+} channels to pressure overload: biochemical and physiological properties of the dihydropyridine receptors in normal and hypertrophied rat hearts. *Journal of Cardiovascular Pharmacology* **12**, 390–396.

NORDIN, C., SIRI, F. & ARONSON, R. S. (1989). Electrophysiologic characteristics of single myocytes isolated from hypertrophied guinea-pig hearts. *Journal of Molecular and Cellular Cardiology* **21**, 729–739.

POWELL, T., TERRAR, D. A. & TWIST, V. W. (1980). Electrical properties of individual cells isolated from adult rat ventricular myocardium. *Journal of Physiology* **302**, 131–153.

SCAMPS, F., MAYOUX, E., CHARLEMAGNE, D. & VASSORT, G. (1990). Calcium current in single cells isolated from normal and hypertrophied rat heart. *Circulation Research* **67**, 199–208.

SEVERS, N. S., SLADE, A. M., POWELL, T., TWIST, V. W. & WARREN, R. L. (1982). Correlation of ultrastructure and function in calcium-tolerant myocytes isolated from the adult rat heart. *Journal of Ultrastructure Research* **81**, 222–239.

TRITTHART, H., LEUDCKE, H., BAYER, R., STIERLE, H. & KAUFMANN, R. (1975). Right ventricular hypertrophy in the cat – an electrophysiological and anatomical study. *Journal of Molecular and Cellular Cardiology* **7**, 163–174.

TSENG, G. N. & HOFFMAN, B. F. (1989). Two components of transient outward current in canine ventricular myocytes. *Circulation Research* **64**, 633–647.

TSENG, G. N., ROBINSON, R. B. & HOFFMAN, B. F. (1987). Passive properties and membrane currents of canine ventricular myocytes. *Journal of General Physiology* **90**, 671–701.

WATANABE, T., DELBRIDGE, L. M., BUSTAMENTE, J. O. & MCDONALD, T. F. (1983). Heterogeneity of the action potential in isolated rat ventricular myocytes and tissue. *Circulation Research* **52**, 280–290.